Int. j. adv. multidisc. res. stud. 2025; 5(1):803-812

Received: 16-12-2024
Accepted: 26-01-2025

International Journal of Advanced Multidisciplinary Research and Studies

ISSN: 2583-049X

Enhancing Control Strategies for Brushless DC Motors: A Case Study on Automotive Power Closing Systems

[1] Abiodun Samuel Oloruntoba, [2] Emmanuel Olalekan Oloruntoba, [3] Samuel Thomas Oladayo, [4] James Adebayo

[1] Department of Electrical Engineering, University of Applied Sciences, Weingarten, Germany
[2] Department of Power Engineering, Environment Planning, Brandenburgische Technische Universität, Germany
[3] Department of Environmental and Resource Management, Brandenburg University of Technology Cottbus-Senftenberg, Germany
[4] Department of Electrical and Electronics, University of Ibadan, Nigeria

DOI: https://doi.org/10.62225/2583049X.2025.5.1.3723
Corresponding Author: **Abiodun Samuel Oloruntoba**

Abstract

Brushless DC (BLDC) motors have emerged as a preferred choice for industrial applications due to their superior efficiency, durability, and low maintenance compared to conventional brushed DC motors. In the automotive sector, particularly in power closing systems, BLDC motors offer significant advantages over brushed counterparts, including reduced mechanical wear and enhanced performance. This study investigates the functionality and dynamic behavior of BLDC motors tailored for automotive power closing applications, focusing on optimizing control strategies and addressing the limitations of existing systems. The research involved validating BLDC motor control algorithms, emphasizing block and sinusoidal commutation methods. Experiments were conducted to analyze the impact of these algorithms on motor performance, including noise levels, dynamic response to polarity changes, and efficiency under varying load conditions. The developed experimental platform allowed comprehensive testing, including noise measurements and the optimization of control software with enhanced library functions. The findings confirm the potential of BLDC motors to meet automotive power closing requirements, with improvements in noise reduction, efficiency, and operational reliability. This study provides a framework for further advancements in BLDC motor control, contributing to the development of more robust and efficient automotive systems.

Keywords: Brushless DC Motor (BLDC), Automotive Power Closing Systems, Motor Control Algorithms, Block and Sinusoidal Commutation, Noise Reduction in Motors, Efficiency Optimization

1. Introduction

The advent of Brushless DC (BLDC) motors represents a pivotal advancement in the evolution of electric motor technology, particularly in industries that demand high efficiency, reliability, and reduced maintenance requirements. Unlike their brushed counterparts, BLDC motors utilize electronic commutation, eliminating mechanical wear points such as brushes and commutators, thereby enhancing longevity and operational performance (Wilson & Trickey, 1962; Chapman, 2005). These advantages have driven the widespread adoption of BLDC motors across various sectors, including industrial automation, consumer electronics, and especially the automotive industry.

In the automotive domain, DC motors play a critical role in numerous applications, ranging from window lifters and sunroof actuators to power closing systems. Traditional brushed DC motors, while cost-effective and simple to control, face significant limitations, including higher maintenance needs, operational inefficiencies, and noise generation due to mechanical commutation (Siemens & Alteneck, 1872; Smith *et al*., 2010; Oloruntoba *et al*., 2024). These constraints have spurred interest in BLDC motors as a viable alternative, particularly in applications where performance, noise reduction, and reliability are paramount.

Power closing systems in modern vehicles—comprising automated mechanisms for doors, rear covers, and compartment closures—demand motors that can operate reliably under varying loads, harsh environments, and tight efficiency constraints. BLDC motors are uniquely suited for these requirements, offering superior torque-to-weight ratios, high-speed operation, and minimal acoustic noise during operation (Anderson *et al*., 2015; Li *et al*., 2020). However, integrating BLDC motors into these systems necessitates a thorough evaluation of their control strategies and dynamic behaviors to ensure compatibility and performance consistency.

The control of BLDC motors relies heavily on advanced commutation techniques, which determine the motor's efficiency, acoustic characteristics, and dynamic response. Among these, block (trapezoidal) and sinusoidal commutation methods have gained prominence. While block commutation is straightforward and computationally efficient, it may introduce torque ripples and noise at lower speeds. Conversely, sinusoidal commutation offers smoother operation with reduced torque ripples but requires precise rotor position sensing and higher computational overhead (Park & Kim, 2018; Zhao *et al*., 2019).

This study aims to investigate the functionality and performance of BLDC motors for automotive power closing applications, addressing the following key objectives:

1. Validate the accuracy and reliability of implemented block and sinusoidal control algorithms under varying load conditions.
2. Examine the motor's response to polarity changes, load fluctuations, and control strategies, focusing on open-loop dynamic behavior.
3. Measure and analyze noise levels generated by different commutation techniques, proposing strategies for noise mitigation.
4. Optimize BLDC control software by introducing novel library functions to enhance compatibility and efficiency.

The research involved designing and implementing an experimental platform, enabling precise measurements of motor characteristics and performance under controlled conditions. The results provide critical insights into the trade-offs between commutation methods, noise generation, and efficiency optimization, offering a framework for deploying BLDC motors in automotive systems. By addressing these objectives, this study contributes to the growing body of knowledge on BLDC motor control, with practical implications for automotive manufacturers seeking to enhance the reliability and performance of power closing mechanisms. The findings also pave the way for further advancements in control algorithms and motor integration, fostering the adoption of BLDC motors in next-generation automotive systems.

2. Materials and Methods

System Setup

Necessary for the experimental verification of the commutation algorithm and the motor behavior, an Experimental set-up has been designed. The Hardware set up for the experimental verification comprises the parts as labeled in the picture below.

Setup and Description

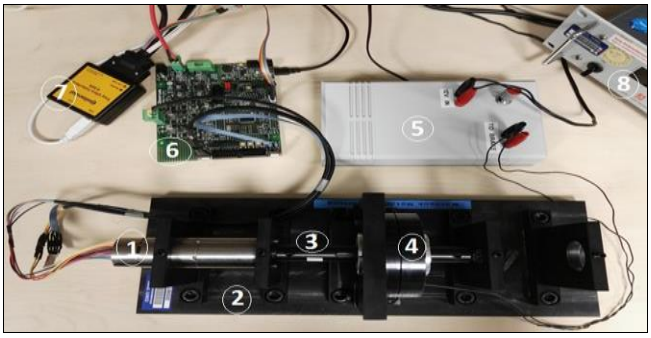

Fig 1: Test System Setup

DUT-Device under Test

1. Mechanical Test Bench
2. Connecting shaft for Drive Motor, Brake and DUT
3. Brake system
4. Brake Controller
5. Motor Controller
6. Measurements Tools
7. Supply voltage.

The Device under Test

The DUT, Faulhaber BLDC motor series 3242G012BX4-4935 has a radial shaft play with two pole pairs. According to the manufacturer, the three-phase brushless Motor has no rotating windings which serve as the basis for the slot-less stator (slot stator is known for cogging) which makes the motor have the following benefits:

- No cogging
- Very High Torque
- High relationship between load and speed, current and torque, and voltage and speed
- Very Low torque ripple.

The Faulhaber motor is housed with an encoder and Hall sensor units in a stainless-steel housing. The inbuilt hall sensor and incremental Encoder are for high-precision position control of the rotor. The Motor can be coupled to a geared system. The motor used in the experiments is coupled to a compatible geared setup which is provided by the manufacturer. All the documented values were carried out at a nominal voltage of 12 V and a room temperature of 22°.

Table 1: Specification of Faulhaber 3242G012BX4-4935, IE3-1024

Quantity	Value	Dimension
Generator constant, KE	2,168	mV/min
Torque constant, KM	20,7	mNm/A
Rotor moment of Inertia	30	gcmˆ2
No of poles pairs	2	-
No of phases	3	-
Rated speed	17000	rev/min
Rated torque	268,7	mNm
Phase to Phase Resistance	0,92	Ohms
Phase to Phase Industance	60	microH
Gear Ratio	66:1	-
Motor+Gear-Lenght	93,6	mm
N/M slope	20,5	-

The three-phase Motor supply wires are No.1 phase -W, NO.2 phase-U, and No.3 phase-V corresponding to the controller board connectors.

The Hall Sensor

The motor is equipped with three hall sensors which are placed 120˚ away from each other in position. The motor came with two sets of cable connections. The first are sets of 8 wires (with different colors) which comprise 3- motor supply lines and 5 cable lines for the Hall signals including the supply and Ground signal. The respective connection to the micro-controller board has to be ensured to avoid a mismatch of signals. Ports J8 is dedicated to all Sensor connectors.

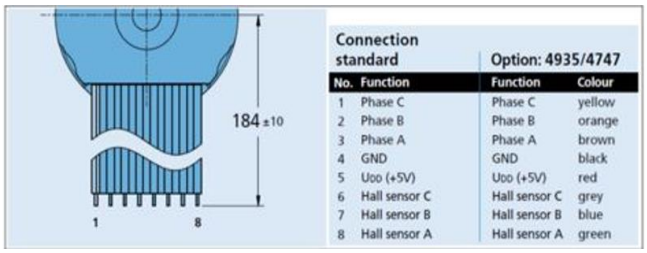

Fig 2: Motor Standard Connections

$$\text{Back EMF constant, } K_E = 2\pi \cdot K_M$$

$$\text{efficiency, } \eta = 1 - \frac{I_0 \cdot R}{U_N}$$

$$\text{No load speed, } n_0 = \frac{U_N - (I_0 \cdot R)}{2\pi \cdot K_M}$$

$$\text{Current constant, } K_I = \frac{1}{K_M}$$

$$\text{N/M slope, } N/M = \frac{R}{(K_M)^2} \cdot \frac{1}{2\pi}$$

$$\text{Stall Torque, } M_H = \frac{(K_M \cdot U_N)}{R} - C_0$$

$$\text{Speed constant, } K_n = \frac{n_0}{U_N - (I_0 \cdot R)} = \frac{1}{K_E}$$

The Encoder

The attached Motor encoder has a resolution of 1024 pulses per revolution. It has 6 - signal cables of which 3 - of them are signal channels (Channels A, B, and I), 1 - supply line (5V), and 1 - Ground line. The rotation direction can be detected by observing the phase shift between the signals A and B. The phase shift between the two signals is set to 90˚. If A leads B by 90˚, rotation is Clockwise (CW) and if B leads A by 90˚ the rotation is Counter Clockwise (CCW). The index signals come up every one complete rotation of 1024 pulses.

Table 2: Encoder Sequence logic

Time	Rotation CH A	clockwise CH B	counter CH A	clockwise CH B
t_1	1	0	0	1
t_2	1	1	1	1
t_3	0	1	0	1
t_4	0	0	0	0

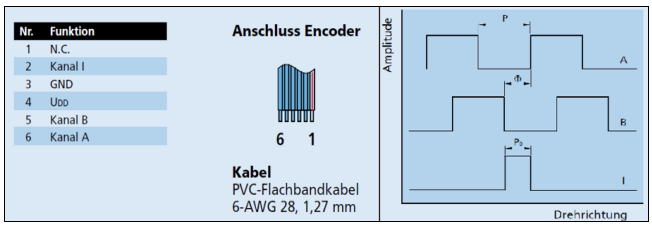

Fig 3: Motor encoder standard Connections [23]

Encoder to Microcontroller Board Connection: The Renesas microcontroller board has a dedicated port for Encoder Channel A and B signals with supply and ground signals, port J9 Connector. The Index signal has been configured and attached to the JPUP1-pin 2 of the microcontroller on the controller Board.

- *The combined gear system*

The above-described Motor is compatible with the Faulhaber planetary-gear series 32/3 with a gear ratio of 66:1 with a maximum efficiency of 70 %. It is rated at 4000 rpm if the motor has to run in a continuous operation mode.

- *Faulhaber Estimation of BLDC Motor Parameter*

Basic equations for determining the characteristics of the motor based on the information provided in the manufacturer's technical documentation are highlighted below:

where J = the moment of inertia R = Phase to Phase resistance K_M = Motor Torque Konstant U_N = Nominal Voltage.

The Device Under Test (DUT) has three interfaces connecting it to the controller board. The interfaces are the Encoder connection ports, the hall sensor connection pins, and the three-phase voltages for the motor commutation.

Test Bench Design

The main aim of the test bench is to provide the possibility of testing and evaluating motor characteristics in the four quadrants of operation. In designing the parts, 3D modeling software (FreeCAD) has been used. This software supports both 3D and 2D representation of the object sketch. However, the realized test bench shown in the picture below has a mounted powder brake that supplies the load torque to the motor shaft or in PC application the door window. Two motors can be attached to the test stand to drive the DUT. The Set up comprises of 12 different parts which have been assembled. These parts include

Table 3: Test bench part list

Part	Quantity	Description
Base plate	1	Main Base plate
		(not shown in picture)
Connecting Plates	5	connects base plate,
		for DUT housing
Base support plates	5	Supports the connecting plate
		and connects it to the Base plate
Connecting Shaft	1	Connects the DUT,
		Drive motor and the Brake system

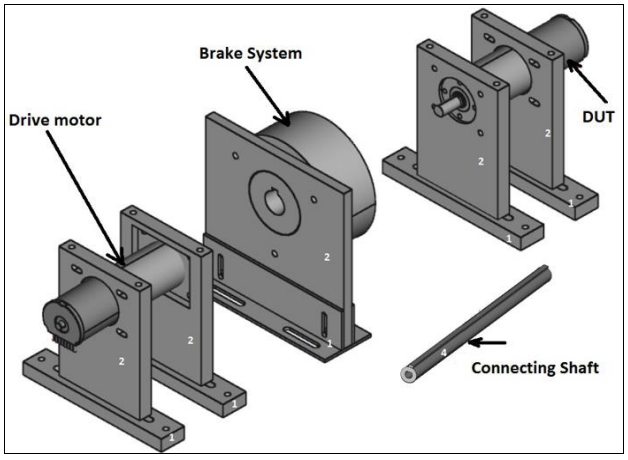

Fig 4: Mechanical Test Bench

Motor Braking

The mounted brake system is a product from the company IBD WICKELTECHNIK GmbH. An electromagnetic powder braking system functions by current inflow to the inner compartments. This current flow makes the braking powder to be active for braking the turning shaft. The braking power output is proportional to the current flow which is controlled by a potentiometer input. This brake system has an internal resistance of 24Ω and a supply voltage of 24VAC.

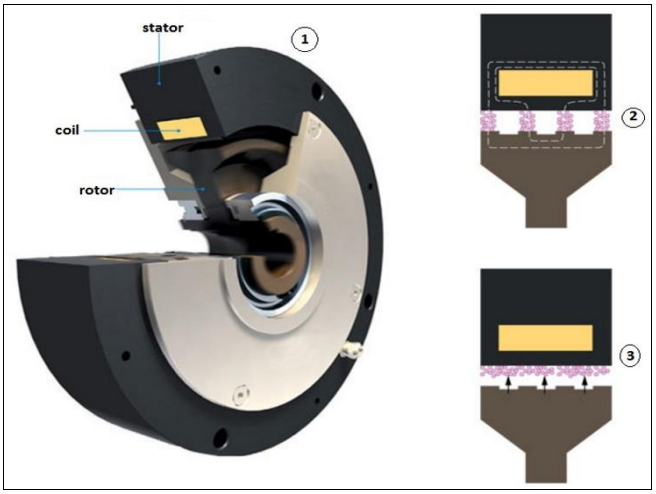

Fig 5: The Powder Brake System

- *Functional Principle:*

The Brake system has three main components Stator, Coil, and Rotor. According to the manufacturer documentation, if current is allowed to flow through the brake system, the magnetic field in the inner coil begins to change directly proportional to the amount of current in the coil. The change in the magnetic field affects the viscosity of the magnetic powder in the gap between the rotor and the stator. If current is on the coil, the powder particles will be magnetized and gathered around the magnetic field lines. The lines are found in the connecting part of the rotor and the stator. The gathered particles between these two-parts cause friction which breaks the rotor (figure 25-2). When the current no longer flows in the coil, the powder magnetization system is reduced and the powder loosens out with a centrifugal force effect for a frictionless rotating system.

Table 4: Technical Data: Magnetic Powder Brake Type B.0055

Characteristics	Value	Dimension
Torque - max	5,0	Nm
Residual - torque	0,04	Nm
Power - supply	24,0	VAC (PWM)
Power - consumption	1,0	A
Resistance at 20°C	24,0	Ohm
Power - dissipation	75,0	W
Weight	1,3	kg
Control -Module - supply	12,0	VDC

From the characteristics curve of the brake. It can be seen that the brake has a non-linear current to Torque output behavior.

BLDC Control Platform

The realized Hardware and software platform for the BLDC control will be discussed here. This Realized BLDC control platform for the Power closing Application has been organized as shown in the picture below:

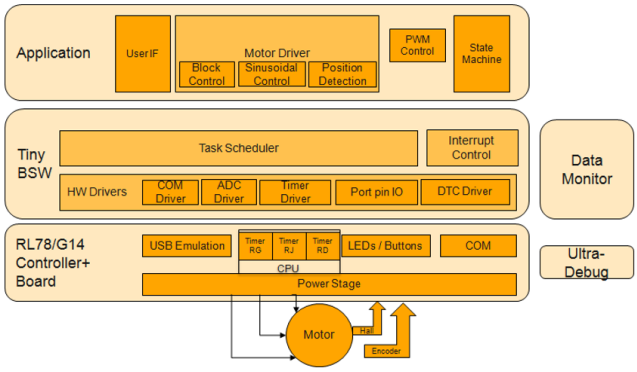

Fig 6: Power Closing BLDCM control Platform

The setup comprises the Application level, the OS level, the Controller level, and the Hardware level. The setup differs from the platform with the current control function. The PI-controller application has been deactivated in this version. It has a new encoder function implemented. The encoder function is controlled by a configured Timer-RG functionality.

3. Results and Discussion

3.1 Results

Experiments and Results

The following experiments were performed:

1. Evaluation of Block and Sinusoidal commutation Algorithms
2. Motor Characteristics -
   1) M/N relationship
   2) Efficiency
   3) Reaction of the motor to Polarity change
3. Acoustic Noise measurements for block and sinusoidal commutation
4. Timer-RG functionality test
5. Verification of Hall sensor Speed with encoder function.

Verification of Commutation algorithms

Here, the commutation done by the hall sensor will be verified. To verify this, a look at the hall sensor input signals and the corresponding output signal on the three-phase voltage output will be done. Commutation errors could result from configuration mistakes in the:

- switching pattern of the Six power MOSFET
- switching pattern of the Hall sensor for commutation.

Assumptions: If there is a commutation error or Phase misalignment,

- Error may result in no output.
- Phase misalignment Error may result in a noisy motor.
- Output phase voltage signals may differ from the ideal signal case.
- by a very large error in Phase misalignment motor current may be very high with a loud Noise and vibration.

If the commutation is done using the encoder, the encoder signal will be used to check this effect by observing the counted value per revolution of the Motor Encoder. This can

be achieved by attaching the encoder index signal to a configured interrupt pin of the microcontroller. This interrupt triggers when the index signal appears and the counted value in the configured Timer-RG for Encoder phase counting can be read.

Block Commutation algorithm

The implemented six step algorithm is given in the Table below,

Table 5: Trapezoidal six step commutation

	State	Hall			U	V	W	U		V		W		TRDOER1
		A	B	C				H	L	H	L	H	L	
Forward	4	1	0	0	-ve	NC	+ve	0	1	0	0	1	0	D7
	6	1	1	0	NC	-ve	+ve	0	0	0	1	1	0	9F
	2	0	1	0	+ve	-1	NC	1	0	0	1	0	0	BD
	3	0	1	1	+ve	NC	-ve	1	0	0	0	0	1	7D
	1	0	0	1	NC	+ve	-ve	0	0	1	0	0	1	6F
	5	1	0	1	-ve	+ve	NC	0	1	1	0	0	0	E7
Reverse	4	1	0	0	+ve	NC	-ve	1	0	0	0	0	1	7D
	5	1	0	1	+ve	-ve	NC	1	0	0	1	0	0	BD
	1	0	0	1	NC	-ve	+ve	0	0	0	1	1	0	9F
	3	0	1	1	-ve	NC	+ve	0	1	0	0	1	0	D7
	2	0	1	0	-ve	+ve	NC	0	1	1	0	0	0	E7
	6	1	1	0	NC	+ve	-ve	0	0	1	0	0	1	6F

Captured signals:

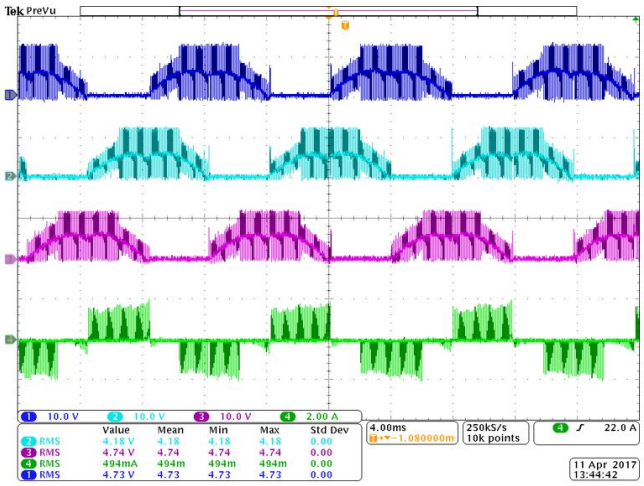

Fig 7: Trapezoidal commutation output signals

The picture above shows one phase voltage on Motor as seen on Channel 1 and its current in channel 4 green color. This test has been carried out in an open loop without PI controller. Thus, characteristics of BLDC operating in this mode is the-same as measured and as described in the ideal case. The motor's speed is proportional to the input duty cycle. Due to the nature of the DUT and the Block commutation technique implemented, cogging was not experienced at lower speed. Alternating Output current can be traced to the Complementary Unipolar PWM supply to the Power electronics devices. As speed increases, the BEMF increases. This effect can also be seen on the amplitude of the current signal as shown in the picture below.

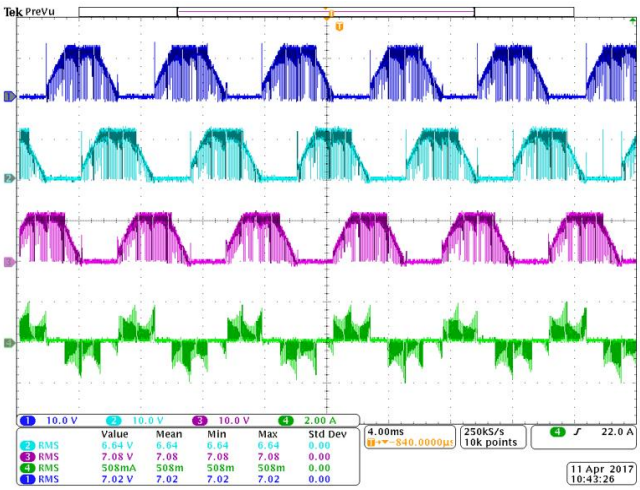

Fig 8: Trapezoidal commutation, EFFECT OF BEMF

3.1.1 Sinusoidal Commutation algorithm

The implemented algorithm as written in the software is summarized in the table below:

Table 6: Sinusoidal six step commutation

	State	Hall			U	V	W	U		V		W		TRDOER1
		A	B	C				H	L	H	L	H	L	
Forward	1	1	0	0	-ve	NC	+ve	0	1	0	0	1	0	67
	2	1	1	0	NC	-ve	+ve	0	0	0	1	1	0	3D
	3	0	1	0	+ve	-1	NC	1	0	0	1	0	0	67
	4	0	1	1	+ve	NC	-ve	1	0	0	0	0	1	97
	5	0	0	1	NC	+ve	-ve	0	0	1	0	0	1	97
	6	1	0	1	-ve	+ve	NC	0	1	1	0	0	0	3D
Reverse	1	1	0	0	+ve	NC	-ve	1	0	0	0	0	1	9D
	2	1	0	1	+ve	-ve	NC	1	0	0	1	0	0	C7
	3	0	0	1	NC	-ve	+ve	0	0	0	1	1	0	C7
	4	0	1	1	-ve	NC	+ve	0	1	0	0	1	0	6D
	5	0	1	0	-ve	+ve	NC	0	1	1	0	0	0	9D
	6	1	1	0	NC	+ve	-ve	0	0	1	0	0	1	6D

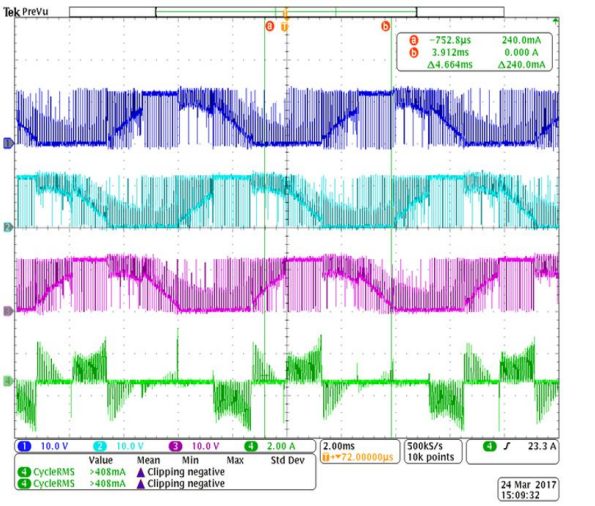

Fig 9: Sinusoidal commutation output signals

The result shows that the implemented sinusoidal algorithm needs to be reviewed for correctness. It can be seen that the Phase voltages and the Current are not looking as in the ideal case. Phase current looks like the trapezoidal commutation current. Expected is a sinusoidal Phase current and bumped shaped sinusoidal phase voltages.

The speed recorded with this algorithm under same duty cycle was higher than the speed recorded using Block commutation under the same condition. So also, is the noise recorded in this sinusoidal commutation mode suppressed.

Observation

The CPU load in the Block commutation mode using Hall sensor, and running Encoder functions at the same time is 78% as shown in the picture below. For a better performance acquiring a microcontroller with a CPU capacity that can allow the implementation of both Sinusoidal and Trapezoidal commutation with Encoder and Hall sensor functionality will be good for a better evaluation of commutation modes.

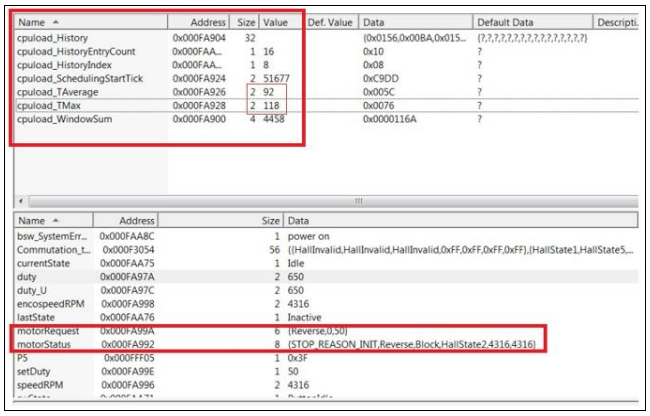

Fig 10: CPU load, measured with Ultra Debug

3.1.2 Verification of Motor Characteristics behavior

To examine the characteristics of a Motor, the load on the motor shaft is increased grad- ually. This results in a slow down of the motor speed. Thus means that, the torque angle becomes larger [31][p352] and the induce torque also becomes larger. Increased Torque implies also that the motor line current increases and speed is reduced. The motor speed at a particular load remains constant but speed reduces with increasing load.

With the following working parameters,

- Input voltage 12V
- PWM Frequency 24KHz
- PWM configuration: Unipolar Complementary mode
- PWM Duty cycle 90%
- commutation mode: Block commutation
- Line Resistance 0.92Ω
- $T_M\,[mNm] = T_m * 66 * 70\%$
- Motor Efficiency based on Equation 39.

Where: Motor Torque (T_m) and Geared Motor Torque (T_M). The following results were collected while investigating the behavior of the motor. The results is based on the Load Torque Equation and Motor Torque Equations 40 and Equa-tion:4.1.2 described above.

Table 7: Duty 90%, Motor Measurement

I_L *A*	*Tload mNm*	N_m *rpm*	T_M *mNm*	V_m *V*	I_m *A*	*P Watt*	*Eff %*
0.00	759.7	5217	420.1	8.1	0.46	3.7	48.51
0.10	1473.4	4444	1051.7	7.7	0.90	7.8	41.32
0.15	1830.3	4026	1349.1	7.7	1.10	8.8	37.43
0.20	2187.1	3773	2133.9	7.6	1.70	12.8	35.08
0.30	2900.8	3448	2915.4	7.5	2.10	15.8	32.06
0.40	3614.5	3092	3867.4	7.4	2.50	18.6	28.75
0.50	4328.2	2816	4855.5	7.6	2.87	21.8	26.18
0.60	5041.8	2678	5390.3	7.4	3.03	22.3	24.90
0.70	5755.5	2553	5896.8	7.5	3.16	23.5	23.74
0.80	6469.2	2459	6277.2	7.4	3.20	23.8	22.56
0.90	7182.9	2281	7226.6	7.2	3.46	24.9	21.21

- *Motor Current behavior*

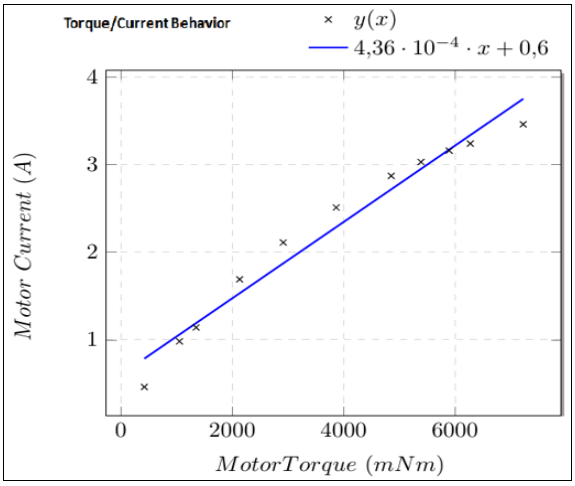

Fig 11: Torque vs Motor Current [35]

- *Geared motor N/M*

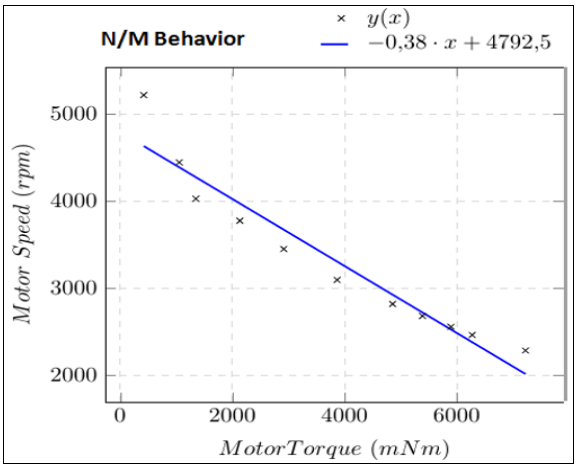

Fig 12: DUT Speed vs Torque characteristics [36]

- *Geared Motor Efficiency*

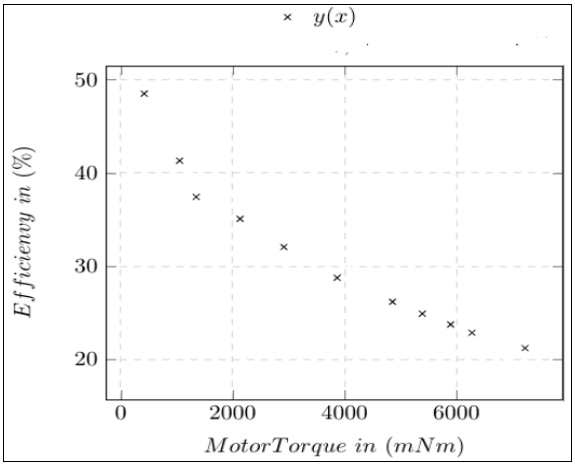

Fig 13: Motor Efficiency

Fig 13 shows the speed response of the DUT as the Torque increases. The highest speed is recorded at no load while the speed decreases as the Torque increases. This relationship is directly proportional to each other and also like in the case of the brushed DC motor speed to Torque behavior. Major

Observation is the non perfectly linear behavior of this relationship because of the load. An approximation of this behavior has a linearity of 93% as shown in the speed/Torque graphic above.

The efficiency of the motor as seen in Fig 14. It can be seen that the efficiency of the motor decreases with increasing Torque. This effect can be traced to the different losses which occurs as motor speed or load on the motor shaft increases.

- *Reaction of motor to Polarity change*

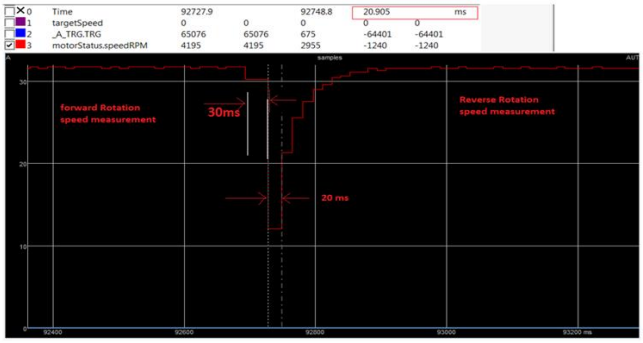

Fig 14: Reaction to direction change[38]

This picture above shows the measurement taken using the Ultra-Debug measurement tool. The motor speed is the red marked profile, which display the maximum motor speed reached in both clockwise and anticlockwise directions of rotation. In this profile, the time it takes the motor to come to stop while rotating in the clockwise rotating direction and change to counterclockwise direction is measured so as to determine how fast the motor reacts to external input. This is regenerative braking method which involve the application of the reverse commutation algorithm to the motor. External input in this case is the direction change button on the controller board.

The reaction time of 30ms to bring geared motor to stop is measured in the forward motoring braking. A time of 20ms has been recorded as the time taken whereby the motor was at rest before direction change starts as seen above. It can also be seen that the speed decreases as soon as the signal to change direction is activated but the short transition time at which the speed reaches zero could not be seen. Responsible for this is the Ultra Debug sampling frequency. It is not fast enough to capture the total speed event frame of the motor.

3.1.3 Acoustic Noise investigation

3.1.3.1 Trapezoidal commutation acoustic noise spectrum

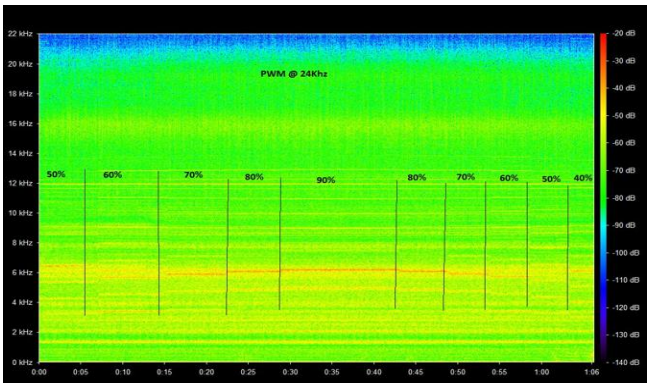

Fig 15: Dutycycle-vs-noise at 24KHz

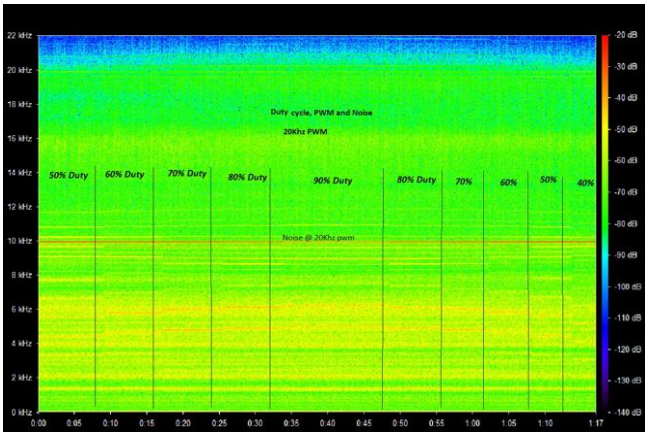

Fig 16: Dutycycle-vs-noise at 20KHz

The above pictures shows the motor noise measured under 20kHz, 24kHz PWM frequency and different Duty Cycle while running motor in Block Mode. At 10KHz, a high peak noise of about -20dB can be seen and at 12KHz a high peak noise of about -35dB can also be seen. This are PWM dependent Noise as it occurs at half of the applied PWM frequency. There are noise harmonics at different frequencies but with a dominant 10 and 20KHz noise visible for at all duty cycle.

In addition, duty cycle or speed dependent noise of about -40dB at lower frequencies or Audible range can also be seen as it varies with the changing motor speed. It consists of noise harmonics.

3.1.3.2 Sinusoidal Commutation acoustic noise spectrum

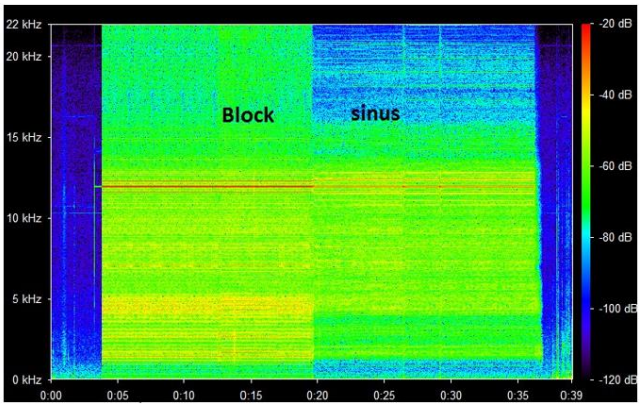

Fig 17: Noise spectrum, Sinusoidal versus Block

The difference between the noise produced by block commutation and sinusoidal com- mutation can be seen as shown in Fig 17 above. Due to the low current consumption of the sinusoidal commutation method implemented in this thesis, the noise associated with block commutation at lower frequency are not seen. Nevertheless, a higher frequency noise can be seen on both commutation methods at the same frequency level. This shows that the source of this noise is dependent on the factors that is peculiar with both com-mutation methods. The major suspect in this respect is the PWM supply and the Hall Sensor used in both commutation modes.

3.1.4 Encoder function test

The picture below is a screen-shot from the Ultra-debug/view image showing the effect of the encoder Index signal at every cycle. The steps represented is the Encoder

channel counter in forward direction. The counter is set to zero at every index signal. This helps to see exactly if the Encoder functions properly.

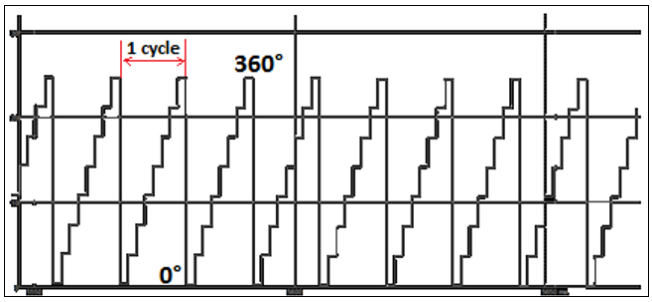

Fig 18: Encoder count and Index Interuption [42]

3.1.5 Hall sensor speed validation with encoder function, and oscilloscope measurement

Further evaluation of the motor using the encoder function has been done. This has been achieved by the comparison of the Oscilloscope measured speed of the motor to the Encoder and the Hall sensor measured speed using the Ultra Debug tool. All measured at the same working point, the following results were recorded.

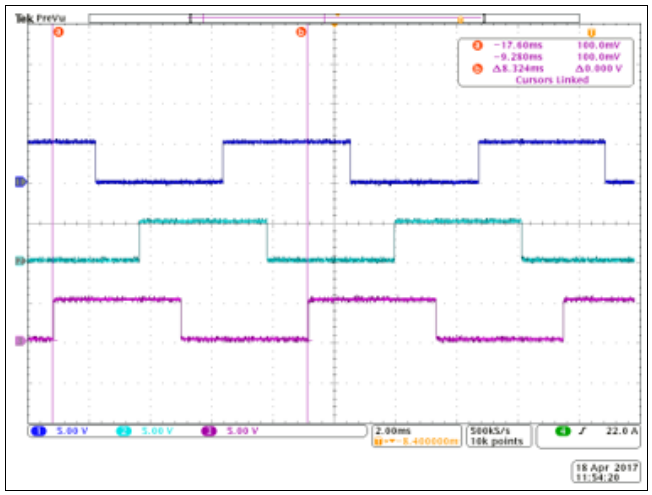

Fig 19: Hall sensor signals

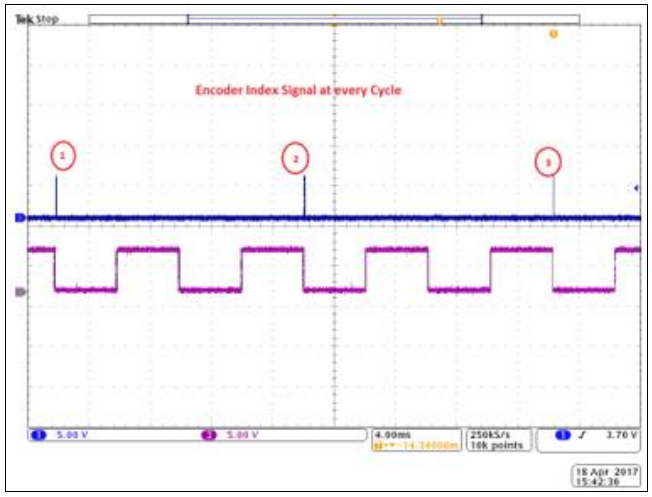

Fig 20: Encoder Index signals

Fig 19 shows the index signal pulse at every motor revolution compared to the hall sensor pulses. The hall pulses has a period of 8.324ms, with a complete rotation time of16.7ms because the rotor has 2-pole pairs of magnet. This measurement gives a resulting revolution speed of 3592.8 in a minute.

$$rpm = \frac{1}{16.7 \cdot 10^{-3}s} \cdot 60s$$

This result confirms the correctness of the speed evaluation using Encoder function and Hall speed. Hall speed The picture blow shows the recorded speed on Ultra-Debug.

Table 8: Motor Speed Evaluation in rpm

Encoderspeed	*Hallspeed*	*measured − Osci*
3592	3592	3592.8

duty_U	0x000FA97C	2	68
encospeedRPM	0x000FA998	2	3592
lastState	0x000FAA62	1	Inactive
motorRequest	0x000FA99A	6	(Forward,0,50)
motorStatus	0x000FA992	8	(STOP_REASON_INIT,Forward, Block ,HallState1,3592,3592)
P5	0x000FFF05	1	0x3F
setDuty	0x000FA99E	1	50
speedRPM	0x000FA996	2	3592

Fig 21: Ultra-Debug Evaluated Motor-Speed

The Ultra-Debug measurement above, shows: The commutation mode used, the direction of motor rotation and the duty cycle applied. So also are the recorded speeds from both the Encoder and Hall sensors included. (Enoguanbhor, *et al*., 2024; Oloruntoba *et al*., 2024; Amos *et al*., 2024a,b).

3.2 Discussion

The results of this study provide valuable insights into the performance and control strategies of Brushless DC (BLDC) motors in automotive power closing applications. The findings highlight critical differences between block and sinusoidal commutation methods, with implications for their application in systems demanding high efficiency and reliability.

3.2.1 Algorithm Performance and Motor Dynamics

The validation of block and sinusoidal commutation algorithms revealed distinct trade-offs between computational simplicity and operational performance. Block commutation demonstrated high computational efficiency and straightforward implementation, making it suitable for cost-sensitive applications. However, the method exhibited pronounced torque ripples and acoustic noise, particularly at low speeds. Conversely, sinusoidal commutation provided smoother torque output and reduced noise levels due to its continuous current waveform. The results emphasize the importance of application-specific considerations when selecting commutation methods.

Dynamic response analysis under various load conditions showed that BLDC motors react predictably to polarity changes, with response times and overshoot influenced by the commutation method and load torque. Fine-tuning control parameters, such as the PWM duty cycle and feedback gain, is essential to achieve optimal performance and minimize transient instabilities.

3.2.2 Acoustic Noise Characteristics

One of the key challenges in automotive applications is noise reduction. The study demonstrated that sinusoidal commutation is superior to block commutation in minimizing acoustic noise, particularly at moderate and low operating speeds. However, noise levels increased at higher speeds due to the limitations of current control loops in

tracking sinusoidal waveforms. These findings underscore the need for advanced control strategies, such as vector control (FOC), to mitigate noise at higher frequencies.

3.2.3 Software Optimization and System Integration

The introduction of modular library functions in the control software proved effective in enhancing system flexibility and scalability. These improvements enable seamless integration of new features and adaptations to meet evolving application requirements. However, hardware limitations, such as insufficient CPU capacity, constrained the implementation of more sophisticated algorithms, such as encoder-based hall sensor emulation. Future upgrades to microcontroller hardware are necessary to fully leverage advanced control techniques.

3.2.4 Implications for Automotive Power Closing Systems

The study establishes BLDC motors as a viable alternative to brushed DC motors for automotive power closing systems, addressing key drawbacks such as maintenance requirements and noise generation. The improved efficiency and reliability of BLDC motors align with industry demands for more robust and durable solutions. Additionally, the ability to optimize commutation methods offers manufacturers the flexibility to tailor motor performance to specific system requirements.

3.2.5 Limitations and Future Directions

Despite the promising results, certain limitations warrant further investigation (Oloruntoba *et al*., 2024). The current study focused on open-loop control and noise analysis, with limited exploration of closed-loop performance under variable environmental conditions. The inability to implement hall sensor emulation due to hardware constraints also restricted the scope of the software optimization. Addressing these limitations through advanced hardware platforms and expanded experimental setups will provide a more comprehensive understanding of BLDC motor performance.

4. Conclusion and Recommendations

This study demonstrates the suitability of Brushless DC (BLDC) motors for automotive power closing applications (Olaniyan and Adegoroye, 2024; Adegoroye *et al*., 2024), addressing the limitations of traditional brushed DC motors. Through comprehensive experimental evaluations, the research validated the effectiveness of block and sinusoidal commutation algorithms and their impact on motor performance, noise generation, and dynamic behavior. The implemented block and sinusoidal control algorithms were successfully validated, showing close agreement between experimental results and theoretical expectations. Block commutation was found to be computationally efficient but prone to torque ripples and noise, especially at lower speeds. Sinusoidal commutation, on the other hand, provided smoother operation with reduced acoustic noise but required higher computational resources and precise position sensing. The open-loop control analysis revealed that BLDC motors exhibit predictable dynamic responses to polarity changes and load fluctuations. However, fine-tuning of the control parameters is essential to mitigate torque overshoot during transient states. Acoustic noise analysis showed that sinusoidal commutation significantly reduces noise levels compared to block commutation. This makes it a preferred choice for applications prioritizing noise reduction, albeit at the cost of increased system complexity. The developed control software was enhanced by introducing modular library functions, enabling greater flexibility for future adaptations and extended functionality on the same platform. Based on the findings of this study, the following recommendations are proposed for further research and practical implementation:

1. Investigate and implement vector control (Field-Oriented Control, FOC) algorithms to achieve higher efficiency and precision in motor control. FOC offers the potential to combine the smooth operation of sinusoidal commutation with reduced computational overhead.
2. Explore sensorless control techniques that utilize back electromotive force (BEMF) to estimate rotor position. This would reduce hardware costs and complexity while maintaining performance.
3. Develop and test advanced noise mitigation techniques, including randomized PWM switching and optimized motor housing designs, to further minimize acoustic disturbances.
4. Expand the study to include other automotive systems, such as seat adjustment motors and window lifters, to evaluate the versatility of BLDC motors across various use cases.
5. Address the limitations of existing microcontrollers by incorporating high-performance processors capable of handling the computational demands of complex algorithms, including sensor fusion for enhanced control accuracy.

5. References

1. Adegoroye A, Ekundayo BP, Olubunmi-Ajayi TS, Amos OO, Olalekan OE. Socio-cultural Drivers of Adaptations and Vulnerability to Climate Change: Lessons from Crop Farmers in Ondo State. International Journal of Agricultural Science, Research & Technology (IJASRT) in Extension & Education Systems. 2024; 14(1).
2. Amos O, Ademola OA, Abiodun OA, Olalekan OE, Opeodu OT, Bode AM. An assessment of municipal solid waste management system in Oshogbo, Osun State Nigeria: Challenges and prospects. International Journal of Multidisciplinary Research and Growth Evaluation. 2024a; 5(1):687-696.
3. Amos O, Abiodun OA, Olalekan O, Opeodu OT, Ademola A. Investigation of Efforts and Problems in Implementing the Basel Convention on the Control of Transboundary Movements of wastes and their Disposal in Nigeria. Asian Journal of Geographical Research. 2024b; 7(1):69-84.
4. Atmel. AVR32723: Sensor field-oriented control for brushless DC motors with AT32UC3B0256, 2016. Retrieved from: Atmel.
5. Doppelbauer M. The invention of the electric motor 1800-1854, 2016. Retrieved from: KIT Institute of Technology.
6. Enoguanbhor Evidence Chinedu, Eveline Aggrey Enoguanbhor, Gladys O Chukwurah, Emmanuel Olalekan Oloruntoba, Iwebuke Edo, Chioma Agatha John-Nsa, *et al*. Spatial Interactions of a City-Region Using GIS and Survey-based Data. East African Journal of Interdisciplinary Studies. 2024; 7(1):176-185.
7. Hughes A. Electric motors and drives: Fundamentals, types, and applications. Newnes, Amsterdam, 2003.

8. Infineon. Cogging torque in a skewed brushless DC motor. Retrieved from Infolytica, 2016.
9. Krishnan R. Electric motor drives: Modeling, analysis, and control. Prentice Hall, United States, 2011.
10. Olalekan OE, Amos OO, Bode AM, James A, Rachel DS. Economic and Operational Feasibility of Biological Methanation in Power-to-Gas Systems: Enhancing Renewable Energy Integration, 2024.
11. Olaniyan OR, Adegoroye A. Bridging Development and Sustainability: An Analysis of the Nigerian Real Estate Sector. European Journal of Theoretical and Applied Sciences. 2024; 2(2):809-823. Doi: https://doi.org/10.59324/ejtas.2024.2(2).72
12. Oloruntoba EO, Oladosu OA, Samuel AA, Bode AM, James A. Optimizing Power-to-Gas Technology for Efficient Renewable Energy Storage and Integration in Germany: A Review. International Journal of Applied and Advanced Multidisciplinary Research. 2024; 2(4):331-356. Doi: https://doi.org/10.59890/ijaamr.v2i4.1656
13. Merz H. Electric machines and drives. VDE Verlag GMBH, Berlin, 2002.
14. Yu J, MonolithicPower. Brushless DC motor fundamentals application note, 2016. Retrieved from: Monolithic Power Systems.